International Journal of Pharmaceutics 570 (2019) 118654

Contents lists available at ScienceDirect

International Journal of Pharmaceutics

journal homepage: www.elsevier.com/locate/ijpharm

Glycine microparticles loaded with functionalized nanoparticles for pulmonary delivery

Amlan Chakraborty[a,b], Simon G. Royce[c,d], Magdalena Plebanski[e,*], Cordelia Selomulya[a,*]

[a] Department of Chemical Engineering, Monash University, Melbourne, VIC 3800, Australia
[b] Department of Immunology and Pathology, Monash University, Melbourne, VIC 3004, Australia
[c] Central Clinical School, Monash University, Clayton, Victoria 3800, Australia
[d] Department of Pharmacology, Monash University, Clayton, Victoria 3800, Australia
[e] School of Health and Biomedical Sciences and Enabling Capability Platforms, Biomedical and Health Innovation, RMIT University, Melbourne, Victoria 3083, Australia

ARTICLE INFO

Keywords:
Glycine microparticle-based excipient
Spray drying
Iron oxide nanoparticles
Inhalation

ABSTRACT

The use of nanoparticles for pulmonary delivery poses challenges such as the presence of anatomical barriers and the loss of bioactive components. Excipients are often used to facilitate delivery. Excipients suitable for nanoparticle delivery are still being explored. Herein we introduce for the first time, spray-dried glycine microparticle-based excipients loaded with nanoparticles of the size range known to be taken up by alveolar macrophages. Using a microfluidic jet spray dryer, we produced glycine microparticles-based excipients which are spherical, uniform, cenospheric (hollow at core), and "coral-like" with average diameter of 60 ± 10 μm, 29 ± 0.8% porosity, and showed their effective loading with glycine coated iron oxide superparamagnetic nanoparticles (GSPIONs). Our loading protocol with nanoparticles further increased microsphere porosity and improved aerodynamic performance unlike the dense, solid commercial excipient, Lactohale200™. This demonstrates a feasible approach for delivery of such nanoparticles in the lung.

1. Introduction

The pulmonary route of drug delivery enables targeting of both local area and systemic circulation by escaping the 'first-pass metabolism' (defined as the loss of a substantial fraction of a bioactive drug before entering systemic circulation, due to its accumulation and processing in the gut and the liver). In addition, pulmonary delivery can improve the stability of compounds, drugs and nanoparticles in the solid-state, at a relatively low product cost. The large alveolar surface area, thin epithelium, and high vascularization of the lungs also maximize drug absorption and hence can help prevent loss of bioactive drugs. Surface functionalized nanoparticles have been used for drug delivery in the lung, with increased drug bioavailability, and capable in some instances of enhanced interaction with target lung resident cells, such as alveolar macrophages (van Rijt et al., 2014). The theoretical optimum location to deposit a drug largely depends on the disease type. For example, drug delivery to the upper airways is needed for asthma while for alveolar lung diseases such as COPD and fibrosis it needs to be delivered deep in the lung (van Rijt et al., 2014). In general particles of size greater than 5 μm are deposited in the trachea while that between 1 and 5 μm are largely phagocytosed and < 1 μm (Carvalho et al., 2011) are deposited in the alveoli (Paranjpe and Müller-Goymann, 2014) for uptake by immune cells. Newer delivery strategies include modifying particle characteristics to change the way they either carry or release the drugs. However, the administration of these nanoparticles poses several problems. Current challenges with pulmonary delivery of some nanoparticles include cytotoxicity, lack of biodegradability, particle instability due to aggregation and/or particle–particle interactions (Yang et al., 2008), and the triggering of damaging pro-inflammatory pathways, amongst other factors (Chakraborty, 2018). Some non-biodegradable nanoparticles can cause the production of reactive oxygen species (ROS) and autophagy leading to the apoptosis of cells (Anozie and Dalhaimer, 2017). Moreover, the accumulation of non-biodegradable or slowly degrading particles can cause chronic inflammation in the region of accumulation (Medina, 2007). Therefore biodegradable particles are usually preferred for pulmonary delivery (Aragao-Santiago, 2016). Although we can overcome these problems, still anatomical barriers such as a narrowing airway lumen as particles travel further out towards the alveoli, and the presence of airway mucus, pose problems. Nearly 25% of ultrafine particles (size < 100 nm) are

Abbreviations: SPION, Super-paramagnetic iron oxide nanoparticles; GSPION, Glycine chemisorbed SPION; API, Active pharmaceutical ingredient

* Corresponding authors.
E-mail addresses: magdalena.plebanski@rmit.edu.au (M. Plebanski), cordelia.selomulya@monash.edu (C. Selomulya).

https://doi.org/10.1016/j.ijpharm.2019.118654
Received 3 April 2019; Received in revised form 28 August 2019; Accepted 30 August 2019
Available online 30 August 2019
0378-5173/

cleared from the lung by mucociliary function in the airways followed by a slower antigen-presenting cell (APC, such as the alveolar macrophage) mediated processes in the lung periphery (Möller, 2008). In COPD patients and smokers, the mucociliary clearance mechanism is impaired due to pulmonary inflammation, with airway remodelling resulting in mucus hypersecretion. However, there are several mechanisms which show incomplete mucociliary clearance, for example, particle displacement due to surface forces caused by surfactants on top of the mucus layer, and of the periciliary fluid towards the epithelium. Moreover, discontinuities in the mucus layer caused by excipients may be capable of reducing local proinflammatory mediators, some of which also promote mucus production. The neutral amino acid glycine has been suggested to have some beneficial properties in this context (Liu et al., 2005; Vargas, 2017), and offers an exciting material to develop useful excipients to use in the lung.

Inhalable biodegradable nanoparticles, as suspensions administered by nebulization, are a growing trend in the pharmaceutical industry (Dailey, 2003), although they have several drawbacks including the inconvenience having to use bulky devices, variability in droplet size (due to nebulizer differences), low delivery efficiency, and the possibility of damage to the active ingredient due to high shear forces (Yang, 2015). A glycine excipient-based system as a dry powder to deliver nanoparticles could offer a useful alternative, due to ease of administration, convenient portability, bulk production, and glycine preventing mucus hypersecretion. Glycine as an excipient is advantageous in terms of cost, availability, low hygroscopicity, excellent physical stability, water solubility along with a sweet taste (Rowe, 2013; Chongprasert et al., 2001). In addition, glycine improves insulin sensitivity along with reduction of alterations induced by hyperglycemia (Nuttall et al., 2002; Alvarado-Vásquez, 2003), by inhibition of oxidative processes (Alvarado-Vásquez, 2003), and has numerous therapeutic benefits such as in treatment of inflammatory bowel disease (Liu et al., 2017), ulcerative colitis (Tsune, 2003), schizophrenia (Javitt, 2001), rheumatoid arthritis (Li, 2001) and inhibiting mucus-producing goblet cells (Liu et al., 2005; Vargas, 2017). This inhibitory effect of D-glycine in preventing mucus production has not been observed in other excipients such as L-glycine or other amino acids, making D-glycine an ideal excipient for the pulmonary delivery of nanoparticles. There has been recent interest also in delivering smaller nanoparticles 10–20 nm to the lung to improve delivery to alveolar macrophages (Feng, 2018; Katsnelson, 2012), a property that has been used to eliminate these cells using nanoparticles loaded with drugs and improve the outcomes from lung cancer in animal models (Ponzoni, 2018). It would, therefore, be advantageous to develop a formulation of glycine excipient-based system as a dry powder capable of encapsulating biodegradable nanoparticles in this size range. Several methods such as spray-drying and freeze-drying can be employed (Liu et al., 2005). However, spray drying is a favored method for development of inhalable dry powder (Yang, 2015; Nandiyanto and Okuyama, 2011) due to its scalability, adaptability, cost, encapsulation efficiency (Sou, 2016) as well as generating uniform, monodisperse particles with higher stability and nanoparticle entrapment capability (Lin, 2017; Wu, 2011). Glycine has been used to encapsulate antibiotics for inhalation, however the dryer used (Buchi 290) generates non-uniform, agglomerates of spray-dried powder due to aerosolization of glycine, instead of even microparticle formation, as could be produced with the much more advanced micro-fluidic jet spray dryer which uses a piezoelectric droplet generator (Lin, 2017; Lin, 2015; Liu, 2011). Using the micro-fluidic jet spray-dryer, we can alter the particles' physicochemical properties including size, distribution, density, shape, morphology without aggregation issues of nanoparticles (Seville et al., 2007), as the nanoparticles are suspended in the bulk excipient (glycine for example). We utilized this principle to design our inhalable spray-dried glycine microparticle-based excipient to carry GSPION to protect them from mucociliary clearance.

In this study, we investigated the feasibility of using a micro-fluidic jet spray dryer to produce inhalable nanoparticles in a glycine-based excipient for pulmonary delivery. Although the use of glycine as a freeze-dried excipient is known in the literature (Liu et al., 2005; Rowe, 2013; Chongprasert et al., 2001; Wang, 2000), these are much larger and pyramidal, with little potential utility as an excipient for lung delivery. Spray-dried glycine microparticles of a suitable size, and aerodynamic performance, as an excipient for embedded biodegradable nanoparticles, have not been explored. Therefore, in this study, we loaded biodegradable super-paramagnetic iron oxide nanoparticles surface-functionalized with glycine (GSPIONs), as model nanoparticles for use with spray-dried glycine excipient. The feasibility (proof of concept) and characterization of the spray-dried excipient in the form of microparticles were evaluated in terms of their aerodynamic properties and GSPIONs encapsulation capability. This work provides a foundation for the use of spray-dried glycine excipient microparticles containing biodegradable nanoparticles for the potential treatment of respiratory diseases, and to study the mechanism of immune cell interactions in the lung.

2. Experimental

2.1. Materials

D-Glycine (ReagentPlus® G7126; ≥99.9% HPLC grade), Iron (II) Chloride, Iron (III) Chloride, ammonium persulfate (A3678, ≥98%), ninhydrin (151173, ACS) was obtained from Sigma-Aldrich. Sodium chloride was obtained from Merck (106404). Phosphate buffered saline (PBS) was prepared in-house by dissolving 2.76 g Sodium dihydrogen phosphate ($NaH_2PO_4{\cdot}H_2O$), 11.35 g Sodium mono-hydrogen phosphate anhydrous ($NaHPO_4$) and 43.76 g sodium chloride (NaCl) in 3L Milli-Q water and pH adjusted to 7.2, followed by making up the volume to 5 L. Ammonia solution 25% (EMSURE®, ISO, Reag. Ph Eur), hydrochloric acid 37% (EMSURE®, ACS, ISO, Reag. Ph Eur) and absolute ethanol (EMSURE®, ACS, ISO, Reag. Ph Eur) was obtained from Merck. Lactohale200™ was purchased from DFE pharma (product code 585686).

2.1.1. Glycine coated iron oxide nanoparticles (GSPIONs)

Glycine coated iron oxide nanoparticles were produced using a modified alkaline co-precipitation procedure as per (Barick and Hassan, 2012). The average diameter of the particles was measured using Quantax analysis system (Delgado, 2007; Ohshima, 1995). The GSPIONs were dispersed with a narrow standard deviation (SD) with an average size of 12 ± 5 nm. XRD analysis revealed the formation of crystalline metastable cubic γFe_2O_3 structure with lattice constant $\alpha = 8.212$ Å. The electron diffraction pattern and the HRTEM image of GSPIONs confirmed the degree of crystallinity of their constituents. The size and structure of GSPIONs for loading onto the microparticles were confirmed by high-resolution transmission electron microscopy (HR-TEM), X-ray diffraction (XRD) and field-dependent magnetization. X-ray Diffraction (XRD) pattern was recorded on a Rigaku Miniflex diffractometer with CuKα radiation and crystal structure were analyzed using the Crystallography Open Database (COD). The infrared spectra were recorded in the range of 4000–450 cm^{-1} on a Fourier Transform Infrared Spectrometer (FTIR, Perkin Elmer Spectrum 100 spectrometer). HR-TEM images were acquired by the FEI Tecnai G2 F20 S-TWIN FEGTEM connected to a wide-angle Orius SCD200D CCD camera. HR-TEM procedures were conducted in the Monash Centre for Electron Microscopy (MCEM). The GSPIONs were biocompatible and did not alter the viability of A549 cell (human adenocarcinomic alveolar basal epithelial cells) at concentrations up to 400 μg/ml (data are shown in supplementary information Fig. 2) when compared to normal/untreated A549 cells. In addition, the GSPIONs suspended in a biological medium (RPMI 1640 + 10% FBS) showed stability in the pH range of 5–8 (data are shown in supplementary information Fig. 3), within the pH range encountered at the respiratory tract from nose to lung (Fischer and Widdicombe, 2006). The efficiency of chemisorption of glycine

onto iron oxide nanoparticles was 38% by extrapolation from a ninhydrin standard curve and HRTEM coupled with EDX mapping for carbon and nitrogen with iron as control.

2.2. Fabrication of glycine microparticle-based excipient for encapsulating GSPIONs

Glycine microparticle-based excipient was fabricated by spray drying using a microfluidic jet spray dryer (Wu, 2011; Liu, 2011) to produce monodisperse particles. This dryer uses a piezoelectric pulse for droplet generation, rendering even droplets. The dryer uses a nozzle of a specific bore diameter. To prevent clogging due to small nozzle bore, a nozzle with a bore diameter of 100 μm was used as it was found to block below this bore-size. An aqueous solution of 8 wt% and 18 wt% glycine was used as precursors for the process. Glycine solution was spray-dried at 173 °C inlet drying temperature. Small amounts of the spray-dried glycine powder were placed in a Petri plate and were stored under dry condition (< 20% RH) or at humid (~76% RH) at room temperature. To reduce the size of glycine micro-carriers, we tried synthesizing them using a commercial spray dryer, Buchi 190 (De Souza et al., 2000) (the detailed procedure can be found in the Supplementary Information 1). However, we discontinued using the Buchi 190 spray drier as it produced non-uniform particles (see Supplementary Information Fig. 1A–C). Hence from this point forward when we mention spray-dried glycine microparticle-based excipient, they were synthesized by the micro-fluidic jet spray dryer.

The GSPIONs were loaded/embedded on to the spherical glycine microparticle-based excipient. In a typical process, 0.01% (w/v) of GSPION dispersed in DI water was used for loading onto the glycine microparticles for spray drying. These GSPIONS were mixed in an aqueous solution of 17.99 wt% glycine. The inlet temperature was maintained at 173 °C. The GSPIONs loaded glycine microparticle-based excipients were kept in a desiccator with silica beads to avoid moisture (as moisture would solubilize the excipient letting out the nanoparticles).

2.3. Morphology and characterization of GSPION encapsulated in glycine microparticle-based excipient

The size, structure and porosity of the microparticle-based excipient were measured using SEM and X-Ray CT. To determine the size and structure of the microparticles a FEI Nova NanoSEM 450 FEGSEM was used with a Bruker Quantax 400 X-Ray analysis system. SEM procedures were conducted in the Monash Centre for Electron Microscopy (MCEM). Images were acquired in both high and low vacuum to obtain high-resolution images at accelerating voltages between 2 kV and 3 kV with spot size 2.0–3.0. To determine the porosity of the microparticles an ultra-high resolution (0.75 μm, Zeiss Xradia XRM520Versa) X-ray Microscopy Facility (Xradia, Pleasanton, CA, USA) was used for image acquisition in this study. Image projections were acquired by rotating the load-stage 360° around its vertical axis. The frame size of the projections was 1024 × 1024 pixels. Scans were performed at 80 kV, 3 W with voxel size 0.75 μm. Voxels are defined here as pores. Scanning parameters used for all the samples were kept consistent for comparison. The 2D projections were reconstructed to 3D volumes. The reconstructed images were post-processed using an image processing software Avizo (V9.1.1, FEI, Hillsboro, OR, USA) (al Mahbub, and Haque, 2016). Images of microparticles were cropped from the whole apparatus assembly followed by removal of noises using appropriate filters. Subsequently, the solid and void phases (pores) of the image were segmented and the voids were measured.

2.3.1. Quantitative and qualitative analysis of spray-dried glycine microparticle-based excipients encapsulating GSPIONs

The GSPION loaded onto spray-dried glycine microparticle-based excipients were analyzed both by Energy Dispersive Xray (EDX) and Thermogravimetric analysis (TGA) to find the location, behaviour and loading of the nanoparticles in the microparticle-based excipient. A Bruker Quantax 400 EDX attached to the Nova SEM was used to map C, N, O and Fe at an accelerating voltage of 15 kV with WD 5.4 mm. To confirm the loading of the GSPIONs into the microparticles, TGA was performed using a Perkin Elmer STA8000 TGA analyser in-between temperatures 50 °C-600 °C. The difference in the degradation profile of the uncoated SPIONs and the GSPION loaded in the microparticle-based excipients were analyzed.

2.3.2. Iron concentration measurement in GSPION-loaded on to glycine microparticle-based excipients

Iron concentration is a direct measurement of the efficiency of encapsulation by the spray-dried glycine microparticles-based excipients. Iron concentration was measured by adapting a method of Rad et al (Rad, 2007) which utilizes the complex formed by ferric ions with the chloride. A standard curve was created by dissolving ferric nitrate in 5 M HCl at concentrations from 1 to 200 μg/ml Fe^{3+} ions. For measuring the concentration of a batch of nanoparticles synthesized, the nanoparticles were dissolved in 5 M HCl and the absorbance at 345 nm based on the standard curve. Ammonium persulfate is dissolved in HCl to oxidize Fe^{2+} ions to Fe^{3+} ions. A microplate reader was used to calculate the absorbance of the assay at 345 nm with a final volume of 100 μL/well. Glycine concentration was measured using a modified ninhydrin assay as glycine was used as a model drug/compound for coating on the nanoparticle surface. An 8% w/v ninhydrin solution was made by dissolving 4 g ninhydrin and dissolving in 50 mL acetone. Standard glycine stock was prepared by dissolving 0.05 g/mL glycine in 1 mL PBS. 50 μL of glycine stock solution was added to the first well and serially diluted to 1/12th of the initial concentration at a final volume of 50 μL. This was used to draw a standard curve to determine the concentration of glycine coated to iron oxide nanoparticles. To determine the concentration of the chemisorbed glycine in the nanoparticles, glycine coated SPIONs suspended in PBS was used in triplicates. 100 μL of ninhydrin reagent was then added to all the wells. The plate was covered with aluminium foil and incubated in a heating block at 95 °C for 15 min. The plate was cooled to RT and 100 μL of 50%v/v ethanol. The absorbance was recorded in a micro-plate reader at 570 nm.

2.3.3. Determination of the aerodynamic performance of GSPION loaded on to spray dried glycine microparticle-based excipients

The aerodynamic performance of glycine microparticle-based excipient was compared with a commercial excipient Lactohale200™ (lactose-pharmaceutical grade), using a Next Generation Impactor (NGI) (Copley Scientific. Nottingham, UK). In addition, a proof of concept for pulmonary delivery of both the excipients was compared where Lactohale200™ is well established as an excipient in commercial dry powder but lacking mucus preventing effects. A pump was used to disperse the particles in air stream which could flow through the instrument and impacted on eight consecutive stages of the impactor. A Ventolin® rotahaler® (Allen + hanburys Respiratory care, GlaxoSmithKline) DPI device was attached to the NGI mouthpiece. Four gelatinous capsules (size 3) were used per sample. Each capsule was filled with 50 mg powder of either spray-dried glycine microparticles-based excipients or with Lactohale200™ (control). Samples containing spray-dried glycine microparticles-based excipients (i.e. spray-dried glycine) were spray-dried with or without the GSPIONs nanoparticles. The powder was discharged from the rotahaler® into the NGI. Using a critical flow controller TPK2000 (Copley Scientific, UK), the airflow was set to 45 L/min for 6 s to mimic 4.5 L of air drawn in human inhalation. After actuation, the contents of the individual stages were washed with 5 mL of PBS and any powder deposit was dissolved and collected. The concentration of glycine was measured by ninhydrin assay against a standard curve (in Section 2.5.2) with each stage per sample taken in triplicates. Data was analyzed as the fraction of the

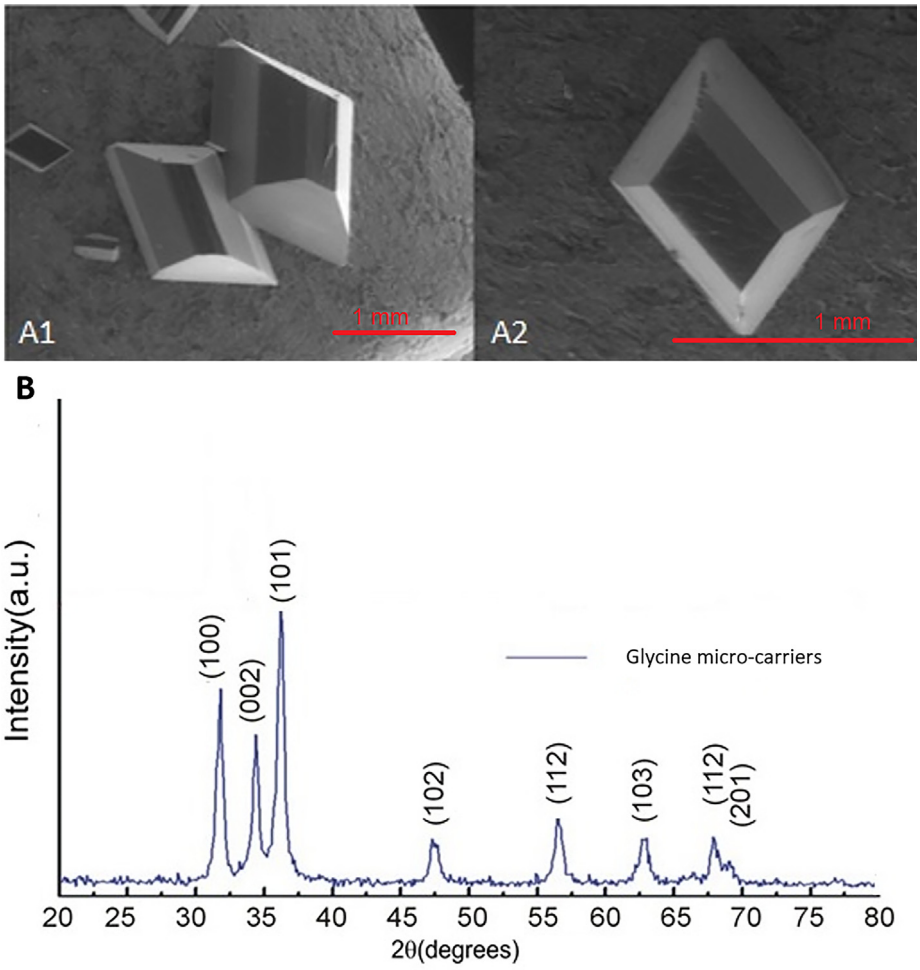

Fig. 1. Commercial glycine and crystallinity of spray died glycine microcarriers. (A) SEM image showing commercially available glycine powder showing bipyramidal shape and 450 μm size; (B) XRD spectra with signature peaks at (1 0 0), (0 0 2) and (1 0 1) of spray-dried glycine microparticles based excipients showing crystallinity of the synthesized microparticles.

recovered dose from 50 mg of loaded sample in the capsule (as excipients form the bulk of any capsule). A two-way ANOVA with post-hoc T-test was used to find significance in between the different samples at different stages.

3. Results and discussion

3.1. Generation of uniform, mono-disperse glycine microparticles-based excipients by microfluidic jet spray drying

Commercially available glycine powder has a size ranging from 450 to 600 μm and is bipyramidal in shape and hence not suitable as excipients for lung delivery (Fig. 1A). The glycine microparticles generated by the microfluidic jet spray dryer were around 60 ± 10 μm and were monodisperse, porous and uniform. This size is similar to the d_{50} values of commercial excipients for use in the lung such as like Lactohale200™, albeit still above the theoretical ideal size suggested size for optimal wide-spread pulmonary delivery (upper respiratory tract < 5 μm, lower respiratory tract 1–5 μm and alveoli < 1 μm) (van Rijt et al., 2014). The main purpose of these glycine microparticles is however as excipients to help prevent mucociliary expulsion of the nanoparticles, and not directly as pulmonary delivery vehicles, making them therefore theoretically also fit-for-purpose. These potential excipient microparticles were therefore further characterized for their surface morphology and structure.

The spray-dried glycine microparticles displayed a spherical shape for all samples (Fig. 2Fig. 2A–D). Crystalline glycine particles produced by cooling or evaporation produces particles which are needle-like, bipyramidal or plate-like (Lin, 2015), and hence may cause airway irritation (Telko and Hickey, 2005), and lead to inflammation (Rydman, 2014; Larsen, 2016), upon use as excipients. However, the bipyramidal shape of the particles (commercially available glycine powder as shown in Fig. 1A) has been transformed to a spherical shape due to the process of spray drying to produce monodisperse particles (Lin, 2017; Lin, 2015). Microparticles with different feed concentrations (8 wt% and 18 wt%) of glycine, displayed similar sizes around 60 μm for the final spherical dry powder formed. The spray-dried microparticles with 18 wt% glycine concentration was dense with a single hole at the point of droplet disengagement (Fig. 2A, B). The microparticles spray dried with 8 wt% glycine concentration displayed a hollow microsphere (Fig. 2C) and a coral-like structure as reported here and previously (Lin, 2015) unlike randomly shaped particles of Lactohale200™. Furthermore, XRD data of the glycine microparticle-based excipients without the GSPIONs, shows three peaks indicating the extent of crystallinity (Fig. 1B). When these microparticles were stored at 76% relative humidity (RH), they became more porous and coral-like (Fig. 2D) indicating that an increase in moisture would lead to the disintegration of the particle. The inlet temperature also played a major role in spray drying. At an elevated temperature of 185 °C, the crystal formed was in large blocks compared to that spray-dried at 173 °C. When the velocity of air during the spray drying process was increased to 400 ms^{-1}, several striations were observed under immersion mode (ultra-high

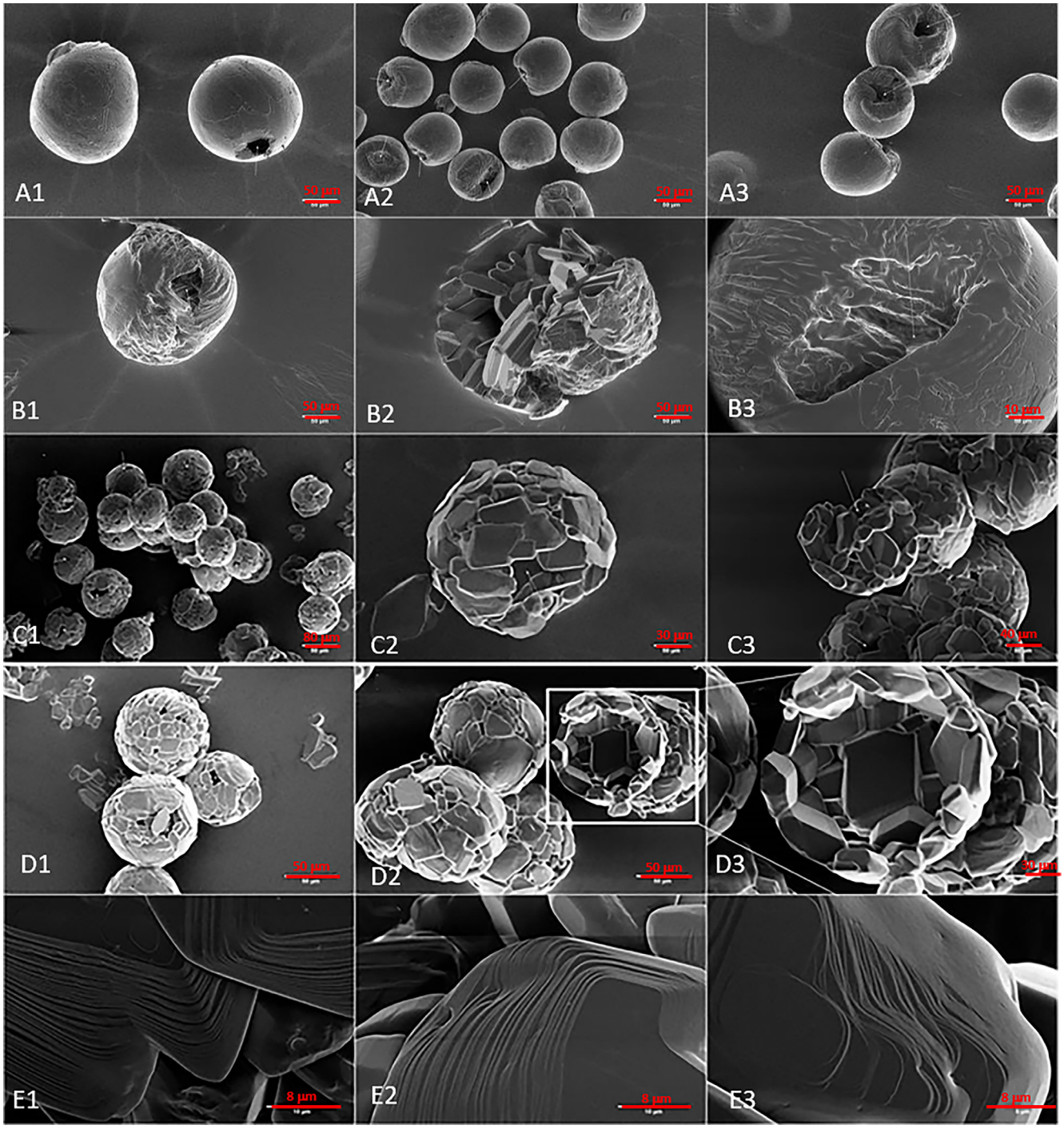

Fig. 2. SEM images of spray-dried glycine microparticle-based excipient synthesized using a microfluidic jet spray drier. (A) Glycine microparticles synthesized with a feed concentration of 18 wt% showing similar spherical shape, uniform but (B) dense, monodispersed having a single large pore; (C) Glycine microparticles synthesized with a feed concentration of 8 wt% showing crystalline, spherical, uniform microparticles with (D) a hollow core (cenospheric) along with a highly porous surface; (E) High resolution image of the microparticle surface showing striation (wave and ridges).

resolution) of the microscope (Fig. 2E). The crystals joined to form the microparticle and is like a cenosphere (hollow shell-like) (Fig. 2D, 2–3). Therefore, the 18 wt% feed concentrations were discontinued and for the rest of the experiments, spray-dried glycine microparticle-based excipients were formed with 8 wt% feed concentration and the excipient particles stored under 76% RH to generate a high degree of porosity. The pores are induced into the particles by humidity treatment due to internal flow of glycine by capillary forces exerted on the condensing water as observed by us previously (Lin, 2015). The introduction of porosity is a key feature for this microparticle-based excipient, rendering them hollow, cenospheric for an improved aerodynamic performance, unlike solid, dense Lactohale200™.

3.2. Characteristic features for spray-dried glycine microparticle-based excipients for pulmonary delivery of GSPIONs

Iron oxide nanoparticles and particularly superparamagnetic iron oxide nanoparticles (SPIONs) are found in many biomedical applications (reviewed in (Chakraborty, 2018). Such nanoparticles are biodegradable as iron oxide nanoparticles are broken down through the

endosomes (Mazuel, 2016) and are non-toxic to cells even at high concentrations, up to 400 μg/ml (Ghasempour, 2015), similar to our observations (Supplementary Information Fig. 2). The magnetic property of the particles can make them useful for use as magnetic resonance imaging (MRI) contrast agents, which could be used in the lung to track pulmonary delivery and potential uptake by lung resident immune cells. Coating iron oxide nanoparticles with amino acids provide stability and can provide improved biocompatibility (Fischer and Widdicombe, 2006). Glycine is a neutral dietary amino-acid as well as a cell preserving agent. We coated iron oxide nanoparticles with glycine using a modified alkaline co-precipitation procedure (Barick and Hassan, 2012), which yielded crystalline superparamagnetic particles (GSPION) in the TEM size range of 12 ± 5 (Feng, 2018; Barick and Hassan, 2012). Recent studies with iron oxide nanoparticles have shown that TEM size of 10 nm is ideal for uptake by macrophages (Feng, 2018) especially alveolar macrophages (Katsnelson, 2012).

To explore a practical way to deliver such nanoparticles into the lungs using a suitable excipient, GSPIONs were loaded at a concentration of 200 μg/ml onto 8 wt% glycine feed concentration to generate microparticle-based excipients. The spray-dried microparticles encapsulating GSPIONs were uniform in size with low standard deviation (Fig. 3A). Upon dissolving the microparticle-based excipients containing the GSPIONs in PBS and quantifying for their iron content, we found the iron concentration to be 2.45 μg/ml. These spray-dried glycine microparticles appeared to be hollow inside (Fig. 3B) making them potentially aerodynamically efficient, unlike solid, dense Lactohale200™ who are current market products. To note, the "coral-like" surface of the microparticle-based excipient changed to a rough surface due to the presence of GSPIONs (Fig. 3C).

We next evaluated the aerodynamic performance of the microparticles-based excipient. The X-ray CT reconstituted 3D images of the glycine microparticles-based excipients containing the GSPIONs (Fig. 4) showed the presence of pores (pointed by arrows) on the outer surface (Fig. 4A) along with a high degree of uniformity in their size (Fig. 4). Moreover, when we observed the cross-section of these microparticles, we found that due to the GSPIONs presence, there was the formation of longitudinal pores (showed by arrows) making the particles very light and aerodynamically efficient (Fig. 4B, Supplementary video 1). We compared our spray-dried glycine microparticle-based excipient with commercial Lactohale200™ for aerodynamic performance which is defined in terms of its porosity, equivalent spherical diameter and aerodynamic volume (Supplementary video 2). We found that our microparticles have a median porosity of 29%, 377439 μm^3 volume and 80 μm aerodynamic diameter. In Lactohale200™, the pores were not detected at our voxel size due to the dense nature of Lactohale200™ which also explains its reported early deposition in the respiratory tract (Hazare and Menon, 2009). Lactohale200™ particles were of non-uniform shape with high poly-dispersity index. The MSDS of Lactohale200™ indicates a physical diameter (d_{50} = 50–100 μm) whereas it is reported in the literature to be around 62.8 μm (Le, 2012). A summary of the comparison between GSPIONs loaded on to glycine microparticles-based excipients versus that of the same excipient without GSPIONs are shown in Table 1.

We also evaluated the location of the GSPIONs using EDX (to validate our XRay CT data) and investigated whether the glycine microparticles used as excipient shields the GSPIONs from degrading by thermogravimetric analysis. Whether the protective effect of using spray drying to form glycine microparticles is extended to other APIs coated on SPIONs, will be of interest to explore in subsequent studies. On examination of the location of the GSPIONs by EDX (Fig. 5A) it was observed that the nanoparticles were located mainly on the inside. Due to the simultaneous effect of drying and crystallization, there is the formation of a wave-like structure (Fig. 3B) and ridges (Fig. 3C) (Islam and Langrish, 2010). Since glycine is an amino acid, the presence of

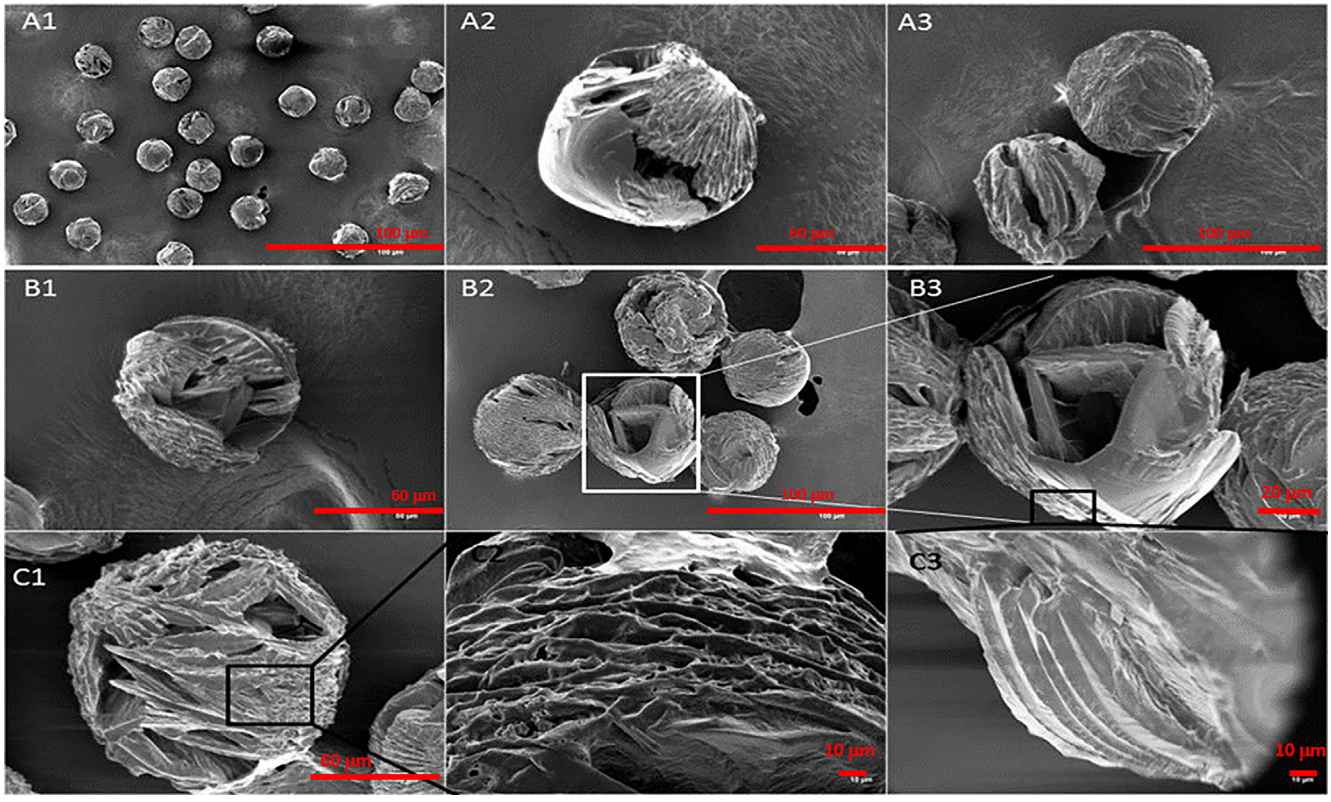

Fig. 3. GSPIONs loaded on to spray-dried glycine microparticles-based excipients. (A) The average size ranged from 60 to 80 μm with both smooth and uneven surface morphology. The spherical structure of the microparticles was maintained. There were several cracks on the crystal (A3). (B) The glycine microparticles-based excipient was found to be rough from inside with wall like growth inside the hollow microsphere (B3). (C) On higher magnification, wave like structure (C2) was observed on the surface which is due to GSPION deposition with ridges marked by high velocity air (C3).

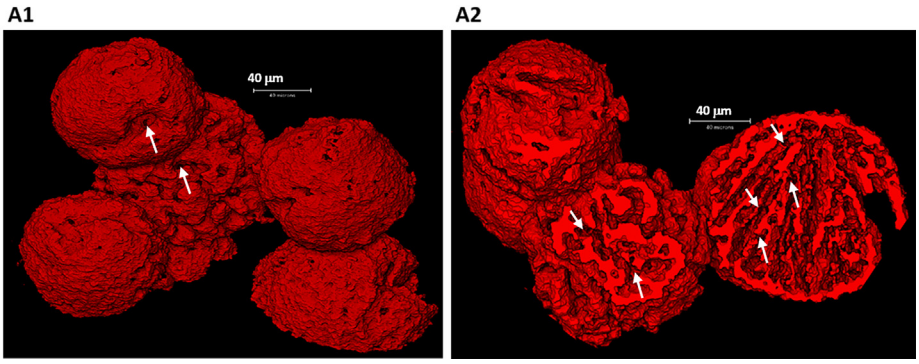

Fig. 4. XRay CT 3D reconstituted images of GSPIONs loaded on to spray-dried glycine microparticles-based excipients (A) Surface of the microparticles showing pores (white arrows) by a voxel size of 0.75 µm with (B) the presence of a highly porous core showing longitudinal pores upon looking into their cross-sections. Inset showing the narrow particle size distribution confirming their uniformity and monodisperse nature. Three representative particles were used for measurement and statistical analysis.

Table 1
Morphometry analysis of Glycine microparticles based excipients and Lactohale200™ for three representative particles per sample.

Sample	Particle Z-axis position	Volume (µm^3)	Equivalent Spherical Diameter (µm)	Porosity (%)
Glycine microparticles based excipients	460–555	305,227.401	83.55	29.45
	456–556	271,511.45	80.45	29.7
	500–598	295,580.39	82.66	29.2
Lactohale200™	393–524	495,553.36	98.2	28.7
	419–540	523,816.03	100.03	29.44
	415–536	537,571.69	100.9	29.38

carbon, nitrogen, oxygen was mapped using the EDX (showed in Supplementary Fig. 1D). However, the microparticles were unstable at a high accelerating voltage of 15 kV (probably due to heat), for EDX, therefore, the inside of the micro-carriers could not be mapped. It can be said that due to fast evaporation there is a bubble formation in the core where the nucleation starts to take place with the GSPIONS serving as a nucleus and concentrating at the core with larger crystal formations (Fig. 3B2-3).

TGA confirmed the loading of the GSPIONs on to the spray-dried glycine microparticles-based excipients. A comparative analysis of spray-dried glycine microparticles-based excipients loaded with GSPIONs, empty glycine microparticles, and GSPIONs by itself were carried out (Fig. 5B). GSPIONs showed negligible weight loss in between 50 °C and 600 °C (the range of temperature analyzed). A two-stage degradation was visible in glycine microparticles and GSPION loaded glycine microparticles. The excipient concentration of glycine used at 8 wt% yields 26% residue due to coke formation under N_2 atmosphere because of pyrolysis. The GSPIONs loaded glycine microparticles had a significant change of weight in between 220 °C and 280 °C which can be due to physisorbed water, making the dissolution of the excipient ideal upon encountering mucus. Both empty and GSPION loaded glycine microparticles-based excipients showed stability from 180 °C to 220 °C and thermal decomposition starting beyond 220 °C irrespective of GSPIONs. There is less mass loss in GSPION

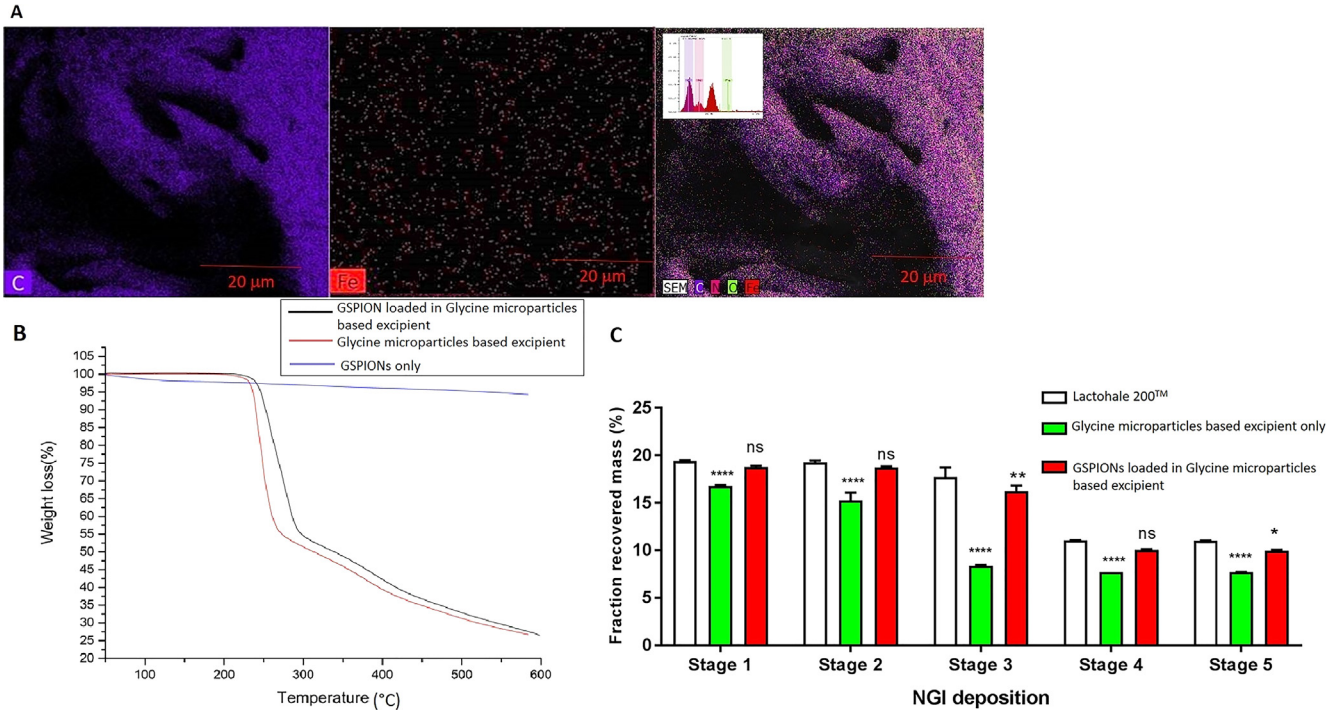

Fig. 5. (A) The location of the GSPIONs was determined by EDX mapping for iron and other elements such as carbon, nitrogen, oxygen. Iron is present relatively at low abundance on the surface which is also confirmed by the peak intensity of the different elements present (inset); (B) Thermogravimetric analysis showing stability and protective nature of spray-dried glycine microparticles-based excipients loaded with GSPIONs, the microparticles only and the GSPIONs alone without the excipient; **(C)** Distribution of glycine microparticles-based excipients loaded with or without GSPIONs in comparison to commercial excipient Lactohale200™ collected from the next generation impactor at various stages. Data represented as Mean ± SD with n = 4 and 3 assay replicates/stage.

loaded glycine microparticles, in comparison to empty glycine microparticles. This signifies that the GSPIONs are protected from degradation by the spray-dried microparticles and serves well as an excipient. Moreover, the degradation from 300 °C to 450 °C was quite significant as there is a release of several gaseous hydrocarbons. This also demonstrates that the GSPIONs are protected by the glycine microparticles from degrading. The presence of the GSPIONs at the core is also confirmed as the GSPIONs themselves have a very small weight loss of 5%. This also confirmed the presence of coating of glycine on the SPION surface.

The NGI dispersion data for glycine microparticle-based excipients with and without GPSIONs as well as the excipient Lactohale200™ are plotted in Fig. 5C. The emitted fraction of Lactohale200™ (78.48 ± 1.28%) was higher than the glycine microparticles-based excipient alone (55.83 ± 1.02%) but were comparable to that of GSPIONs loaded on to glycine microparticles-based excipients (73.76 ± 0.98%). The fraction/ratio of recovered powder at stages 1–5 were ($0.194 \pm 7.8 \times 10^{-4}$, $0.192 \pm 1.7 \times 10^{-3}$, $0.177 \pm 9.9 \times 10^{-3}$, $0.11 \pm 2.7 \times 10^{-4}$, $0.11 \pm 7.2 \times 10^{-5}$) for Lactohale200™ which is similar to our GSPIONs loaded glycine microparticles as excipients ($0.188 \pm 1.5 \times 10^{-3}$, $0.187 \pm 1.1 \times 10^{-3}$, $0.162 \pm 5.7 \times 10^{-3}$, $0.101 \pm 5.9 \times 10^{-4}$, $0.099 \pm 7. \times 10^{-4}$). Inspection of the NGI data showed that the majority of the particles deposited in decreasing order from stages 1–5. The maximum glycine microparticle based excipients deposited in stage 1 and 2 was 9.37 ± 0.07 mg and 9.36 ± 0.05 mg whereas for Lactohale200™ it was measured to be 9.69 ± 0.04 mg and 9.63 ± 0.08 mg. This suggests that the majority of the excipients (both glycine microparticles and Lactohale200™) are deposited in the pharynx and the trachea. The particles deposited beyond stage 5 were almost negligible and beyond the detection limit of the assay (data not shown). Spray-dried glycine microparticles-based excipient without GSPIONs majorly deposited in between stage 1 and 2 and limited availability was observed in between stage 3–5. When we compared spray-dried glycine microparticles-based excipients with GSPIONs to that of Lactohale200™ at individual stages, it was found that at stage 1, 2 and 4, there is no significant difference in their deposition between Lactohale200™ and GSPIONs loaded on to glycine microparticles-based excipients. Whereas, the glycine microparticles-based excipients without the GSPIONs were significantly less deposited across all the stages. This deposition is related to the porosity of the microparticles as observed before. The glycine microparticle-based excipient was found to be highly porous (29% porosity from X-ray CT data, refer to Fig. 4), crystalline (refer to Fig. 1B), wave-ridge, “coral-like”, cenospheric (hollow core, refer to Figs. 2 and 3) micro-carriers with aerodynamic diameter (80 ± 10 μm, from 3D reconstruction of XRay CT images) generated during spray drying with GSPIONs. At a flow rate of 45 L/min which is the normal inspiratory flow rate in a human (with a pulmonary disease such as COPD or fibrosis), the microparticles-based excipient carrying the GSPIONs demonstrate a proof of concept that they can travel longer whereas the microparticles alone are carried less due to reduced porosity although both the structures show spherical morphology. Processing of the NGI data also allowed us to compare between the mass median diameter of the microparticles (80 ± 10 μm) in comparison to large physical diameters (d_{50} = 50–100 μm) values of commercial Lactohale200™. The aerodynamic size of the GSPION loaded onto glycine microparticles-based excipient and the d_{50} value of Lactohale200™ coincide and can be correlated with the limited deposition at the different stages of the impactor. Therefore, the microparticles-based excipient has similar aerodynamic performance and capable of pulmonary administration of the GSPIONs. The fabricated glycine microparticle-based excipients have better aerodynamic performance despite having large geometric diameter because of their low densities. The low density of glycine (8 wt%) used as feed concentration to generate the microparticles, owed to cenospheric, highly porous morphologies, causing their aerodynamic diameter to lie within the range for effective depositions past the oropharyngeal region. In addition, the solubility of glycine microparticles-based excipient (240 mg/ml) was higher than that of Lactohale200™ (190 mg/ml) at 25 °C, owing to its porous nature and availability of physisorbed water.

An advantage of the glycine microparticle excipient system for nanoparticle delivery is that, due to the porosity and aerodynamic performance of the microparticles, they can be delivered to the upper airways past the oropharyngeal region, protecting the GSPIONs from the mucus layer. Humidity subsequently will induce partial dissolution of the glycine and subsequent recrystallization. The free energy is proportionally related to crystal area, and therefore small crystal grains tend to grow into larger ones with the ultrafine grains showed in high-resolution SEM images forming larger crystal grains (Lin, 2015). This phenomenon is important to generate discontinuities in the mucus layer, as well as to release the GSPIONs after impact, for their subsequent periciliary flow towards the smaller airways, and subsequently into the peripheral lung. The released GSPIONs, could be further promoted to localize to specific alveolar regions if so desired, by application of an external magnet, as described by Swai and colleagues (Swai, 2009).

4. Conclusion

In summary, our data suggest that spray-dried glycine microparticles synthesized using a micro-fluidic jet spray dryer could be a very useful excipient for the pulmonary delivery of functionalized nanoparticles. These novel glycine microparticle excipients are porous, aerodynamically stable, monodisperse and uniform, which offers advantages over other available commercial excipients in terms of availability, cost of production, ease of encapsulation, homogeneity, hygroscopicity and in preventing mucus clearance for pulmonary delivery.

Using this excipient to encapsulate functionalized super-paramagnetic iron oxide nanoparticles coated with glycine (GSPIONs) is beneficial for use as carriers for pulmonary delivery. The GSPIONs tested are of the reported size ideal for uptake by lung resident immune cells, neutrophils and alveolar macrophages. Overall, these data demonstrate that spray-drying can be used to design inhalable, biodegradable microparticle-based excipient system for protecting and/or encapsulating functional nanoparticles for pulmonary delivery. It also provides future directions to deliver these nanoparticles as therapeutics in the attenuation of airway inflammation. Our findings provide new insights into spray-drying of amino acids to design uniform, monodisperse excipients capable of passing the oropharyngeal region for pulmonary drug delivery and supports the hypothesis to deliver inhalable surface-functionalized nanoparticles in the lung periphery without entrapment in the mucus. Finally, our findings suggest the possible use of lung-specific particulate vaccines, drug delivery systems, and immunomodulators. The nanoparticles are inhalable as a dry powder inhaler formed using spray-dried glycine microparticle based excipient, which increases patient comfort and provides a better logistical way for efficient, routine drug administration.

CRediT authorship contribution statement

Amlan Chakraborty: Investigation, Methodology, Validation, Formal analysis, Writing - original draft, Writing - review & editing, Visualization. **Simon G. Royce:** Methodology, Validation, Writing - review & editing, Supervision. **Magdalena Plebanski:** Conceptualization, Resources, Writing - review & editing, Visualization, Supervision, Funding acquisition. **Cordelia Selomulya:** Conceptualization, Methodology, Validation, Formal Analysis, Resources, Writing - review & editing, Visualization, Supervision, Project administration, Funding acquisition.

Funding sources

This project is supported by the Australian Research Council (ARC)

under the Discovery program (DP150101058).

Declaration of Competing Interest

The authors declare that they have no known competing financial interests or personal relationships that could have appeared to influence the work reported in this paper.

Acknowledgments

Magdalena Plebanski is an NHMRC Senior Research Fellow and Cordelia Selomulya is an ARC Future Research Fellow. Mr. Amlan Chakraborty is supported by a co-funded Monash Graduate Scholarship. The authors would like to thank Monash Centre for Electron Microscopy, X-Ray CT facility (Department of Civil Engineering), and the Perkin Elmer Facility, Monash University for the use of their facilities.

Appendix A. Supplementary data

Supplementary data to this article can be found online at https://doi.org/10.1016/j.ijpharm.2019.118654.

References

al Mahbub, A., Haque, A., 2016. X-ray computed tomography imaging of the microstructure of sand particles subjected to high pressure one-dimensional compression. Materials 9 (11), 890.
Alvarado-Vásquez, N., et al., 2003. Effect of glycine in streptozotocin-induced diabetic rats. Comp. Biochem. Physiol. C: Toxicol. Pharmacol. 134 (4), 521–527.
Anozie, U.C., Dalhaimer, P., 2017. Molecular links among non-biodegradable nanoparticles, reactive oxygen species, and autophagy. Adv. Drug Deliv. Rev. 122, 65–73.
Aragao-Santiago, L., et al., 2016. Compared in vivo toxicity in mice of lung delivered biodegradable and non-biodegradable nanoparticles. Nanotoxicology 10 (3), 292–302.
Barick, K.C., Hassan, P.A., 2012. Glycine passivated Fe3O4 nanoparticles for thermal therapy. J. Colloid Interface Sci. 369 (1), 96–102.
Carvalho, T.C., Peters, J.I., Williams, R.O., 2011. Influence of particle size on regional lung deposition – What evidence is there? Int. J. Pharm. 406 (1), 1–10.
Chakraborty, A., et al., 2018. Amino acid functionalized inorganic nanoparticles as cutting-edge therapeutic and diagnostic agents. Bioconjug. Chem. 29 (3), 657–671.
Chongprasert, S., Knopp, S.A., Nail, S.L., 2001. Characterization of Frozen Solutions of Glycine. J. Pharm. Sci. 90 (11), 1720–1728.
Dailey, L.A., et al., 2003. Nebulization of biodegradable nanoparticles: impact of nebulizer technology and nanoparticle characteristics on aerosol features. J. Control. Release 86 (1), 131–144.
De Souza, K.C.B., et al., 2000. The Adjuvants Aerosil 200 and Gelita-Sol-P influence on the technological characteristics of spray-dried powders from Passiflora edulis var. flavicarpa. Drug Dev. Ind. Pharm. 26 (3), 331–336.
Delgado, A.V., et al., 2007. Measurement and interpretation of electrokinetic phenomena. J. Colloid Interface Sci. 309 (2), 194–224.
Feng, Q., et al., 2018. Uptake, distribution, clearance, and toxicity of iron oxide nanoparticles with different sizes and coatings. Sci. Rep. 8 (1), 2082.
Fischer, H., Widdicombe, J.H., 2006. Mechanisms of acid and base secretion by the airway epithelium. J. Membr. Biol. 211 (3), 139–150.
Ghasempour, S., et al., 2015. Investigating the cytotoxicity of iron oxide nanoparticles in in vivo and in vitro studies. Exp. Toxicol. Pathol. 67 (10), 509–515.
Hazare, S., Menon, M., 2009. Improvement of inhalation profile of DPI formulations by carrier treatment with magnesium stearate. Indian J. Pharm. Sci. 71 (6), 725–727.
Islam, M.I.U., Langrish, T.A.G., 2010. An investigation into lactose crystallization under high temperature conditions during spray drying. Food Res. Int. 43 (1), 46–56.
Javitt, D.C., et al., 2001. Adjunctive high-dose glycine in the treatment of schizophrenia. Int. J. Neuropsychopharmacol. 4 (4), 385–391.
Katsnelson, B.A., et al., 2012. Interaction of iron oxide Fe3O4 nanoparticles and alveolar macrophages in vivo. Bull. Exp. Biol. Med. 152 (5), 627–629.
Larsen, S.T., et al., 2016. Airway irritation, inflammation, and toxicity in mice following inhalation of metal oxide nanoparticles. Nanotoxicology 10 (9), 1254–1262.
Le, V.N.P., et al., 2012. Dry powder inhalers: study of the parameters influencing adhesion and dispersion of fluticasone propionate. AAPS PharmSciTech 13 (2), 477–484.
Li, X., et al., 2001. Dietary glycine prevents peptidoglycan polysaccharide-induced reactive arthritis in the rat: role for glycine-gated chloride channel. Infect. Immun. 69 (9), 5883–5891.
Lin, R., et al., 2015. On the formation of “coral-like” spherical α-glycine crystalline particles. Powder Technol. 279, 310–316.
Lin, R., et al., 2017. Spray drying of mixed amino acids: the effect of crystallization inhibition and humidity treatment on the particle formation. Chem. Eng. Sci. 167, 161–171.
Liu, W., et al., 2011. A single step assembly of uniform microparticles for controlled release applications. Soft Matter 7 (7), 3323–3330.
Liu, W., Wang, D.Q., Nail, S.L., 2005. Freeze-drying of proteins from a sucrose-glycine excipient system: effect of formulation composition on the initial recovery of protein activity. AAPS PharmSciTech 6 (2), E150–E157.
Liu, Y., Wang, X., Hu, C.A., 2017. Therapeutic potential of amino acids in inflammatory bowel disease. Nutrients 9 (9).
Mazuel, F., et al., 2016. Massive intracellular biodegradation of iron oxide nanoparticles evidenced magnetically at single-endosome and tissue levels. ACS Nano 10 (8), 7627–7638.
Medina, C., et al., 2007. Nanoparticles: pharmacological and toxicological significance. Br. J. Pharmacol. 150 (5), 552–558.
Möller, W., et al., 2008. Deposition, retention, and translocation of ultrafine particles from the central airways and lung periphery. Am. J. Respir. Crit. Care Med. 177 (4), 426–432.
Nandiyanto, A.B.D., Okuyama, K., 2011. Progress in developing spray-drying methods for the production of controlled morphology particles: from the nanometer to submicrometer size ranges. Adv. Powder Technol. 22 (1), 1–19.
Nuttall, F.Q., Nuttall, J.A., Gannon, M.C., 2002. The metabolic response to ingested glycine. Am. J. Clin. Nutr. 76 (6), 1302–1307.
Ohshima, H., 1995. Electrophoresis of soft particles. Adv. Colloid Interface Sci. 62 (2), 189–235.
Paranjpe, M., Müller-Goymann, C.C., 2014. Nanoparticle-mediated pulmonary drug delivery: a review. Int. J. Mol. Sci. 15 (4), 5852–5873.
Ponzoni, M., et al., 2018. Enhancement of Tumor Homing by Chemotherapy-Loaded Nanoparticles. Small 14 (45), 1802886.
Rad, A.M., et al., 2007. Measurement of quantity of iron in magnetically labeled cells: comparison among different UV/VIS spectrometric methods. Biotechniques 43 (5), 627–636.
Rowe, Raymond C., Sheskey, P.J., Quinn, Marian E., 2013. Handbook of Pharmaceutical Excipients, seventh ed. Pharmaceutical Development and Technology (2): p. 544-544.
Rydman, E.M., et al., 2014. Inhalation of rod-like carbon nanotubes causes unconventional allergic airway inflammation. Part. Fibre Toxicol. 11 48-48.
Seville, P.C., Li, H.-Y., Learoyd, T.P., 2007. Spray-dried powders for pulmonary. Drug Delivery 24 (4), 307–360.
Sou, T., et al., 2016. Designing a multi-component spray-dried formulation platform for pulmonary delivery of biopharmaceuticals: the use of polyol, disaccharide, polysaccharide and synthetic polymer to modify solid-state properties for glassy stabilisation. Powder Technol. 287, 248–255.
Swai, H., et al., 2009. Nanomedicine for respiratory diseases. Wiley Interdiscip. Rev. Nanomed. Nanobiotechnol. 1 (3), 255–263.
Telko, M.J., Hickey, A.J., 2005. Dry powder inhaler formulation. Respiratory Care 50 (9), 1209–1227.
Tsune, I., et al., 2003. Dietary glycine prevents chemical-induced experimental colitis in the rat. Gastroenterology 125 (3), 775–785.
van Rijt, S.H., Bein, T., Meiners, S., 2014. Medical nanoparticles for next generation drug delivery to the lungs. Eur. Respir. J. 44 (3), 765–774.
Vargas, M.H., et al., 2017. Effect of oral glycine on the clinical, spirometric and inflammatory status in subjects with cystic fibrosis: a pilot randomized trial. BMC Pulm. Med. 17 (1) 206-206.
Wang, W., 2000. Lyophilization and development of solid protein pharmaceuticals. Int. J. Pharm. 203 (1), 1–60.
Wu, W.D., et al., 2011. Assembly of uniform photoluminescent microcomposites using a novel micro-fluidic-jet-spray-dryer. AIChE J. 57 (10), 2726–2737.
Yang, X.-F., et al., 2015. The influence of amino acids on aztreonam spray-dried powders for inhalation. Asian J. Pharm. Sci. 10 (6), 541–548.
Yang, W., Peters, J.I., Williams, R.O., 2008. Inhaled nanoparticles—a current review. Int. J. Pharm. 356 (1), 239–247.